Export pathways for river discharged fresh water in the northern Gulf of Mexico

Steven L. Morey,[1] Paul J. Martin,[2] James J. O'Brien,[1] Alan A. Wallcraft,[2] and Jorge Zavala-Hidalgo[1]

Received 4 October 2002; revised 3 March 2003; accepted 15 July 2003; published 1 October 2003.

[1] A numerical simulation of the Gulf of Mexico (GoM) using the Navy Coastal Ocean Model (NCOM) is used to identify the pathways by which fresh water discharged by major rivers in the northern Gulf is exported away from the region. The NCOM, a new primitive equation ocean model with a hybrid sigma/geopotential level vertical coordinate, is described along with its application to the GoM region. Trajectories from surface drifters are analyzed to show evidence of the seasonally shifting alongshore and cross-shelf transport in the region. The model results are used to determine the preferred locations and times of year for cross-shelf and along-shelf export of low-salinity water from the northern GoM. The annual cycle of local wind stress plays an important role in shifting the export pathway of the fresh water discharged from the major rivers (primarily the Mississippi River) toward the east in the spring/summer, where it can be transported offshore by the currents associated with deep ocean mesoscale eddies, and toward the west in the fall/winter, where it is transported southward along the Mexican coastline as a coastally trapped current. *INDEX TERMS:* 4219 Oceanography: General: Continental shelf processes; 4255 Oceanography: General: Numerical modeling; 4243 Oceanography: General: Marginal and semienclosed seas; *KEYWORDS:* cross-shelf transport, fresh water, Gulf of Mexico

Citation: Morey, S. L., P. J. Martin, J. J. O'Brien, A. A. Wallcraft, and J. Zavala-Hidalgo, Export pathways for river discharged fresh water in the northern Gulf of Mexico, *J. Geophys. Res.*, *108*(C10), 3303, doi:10.1029/2002JC001674, 2003.

1. Introduction

[2] The circulation in the Gulf of Mexico (GoM) is dominated by the energetic Loop Current (LC) and its associated eddies. Large anticyclones, called Loop Current Eddies (LCEs), aperiodically pinch off from the LC at intervals from 3 to 17 months [*Sturges and Leben*, 2000] and drift generally westward, where they decay against the continental margin. Associated with the LC and the large anticyclones are a wealth of smaller cyclonic and anticyclonic eddies interacting in a seemingly chaotic manner [*Zavala-Hidalgo et al.*, 2003a]. These features have vertical scales from several hundred to 1000 m and thus remain offshore of the continental shelf.

[3] Wind patterns over the northern GoM are typified by light southeasterly winds during the summer, with frequent cold fronts shifting the mean winds to northeasterly and northerly during the fall and winter. The influence of local wind stress on the GoM circulation is small compared to the energetic LC-induced circulation, but is a dominant mechanism for driving the circulation over the inner shelf.

[4] Filaments and lenses of low-salinity water have been observed throughout the Gulf. The source of this low-salinity water is fresh water discharged to the Gulf from large rivers, primarily from the Mississippi River. The Mississippi River has an annual mean discharge of over 13,000 m^3/s (as measured by the U. S. Geological Survey gauging station 7374000), with the neighboring Atchafalaya River contributing about half as much fresh water to the region as the Mississippi.

[5] Some studies have been conducted to explain the seasonal variability of the shelf circulation to the west of the Mississippi Delta [*Cochrane and Kelly*, 1986; *Vastano et al.*, 1995; *Cho et al.*, 1998], but in less detail to the east [*Chuang et al.*, 1982; *Schroeder et al.*, 1985, 1987]. These works consist primarily of regional observational efforts. The variability of spatial and temporal patterns of salinity has been discussed, with emphasis placed on the advection of the salinity, the varying discharge rates of the major rivers, and the interaction of the pool of relatively fresh water with the deep water mesoscale eddies and the LC [*Brooks and Legeckis*, 1982; *Gilbes et al.*, 1996; *Sahl et al.*, 1997].

[6] Cross-shelf transport has been a topic of much discussion, as it relates closely to the biology of the region, and to pollutant dispersal. The primary mechanism for cross-shelf transport seems to be the interaction of the mesoscale eddies of the Gulf with the shelf water. *Ohlmann et al.* [2001] use a collection of surface drifter data with satellite altimetry to highlight the regions of cross-shelf transport in the Gulf of Mexico. This work suggests that there are "hot spots" for cross-shelf exchange in the northwest and north-

[1]Center for Ocean-Atmospheric Prediction Studies, Florida State University, Tallahassee, Florida, USA.
[2]Naval Research Laboratory, Stennis Space Center, Mississippi, USA.

0148-0227/03/2002JC001674$09.00

east corners of the Gulf, and south of the Louisiana/Texas (LATEX) Shelf. Since these regions are also highly influenced by fresh water discharged from the major rivers in the region, they may serve as pathways of exporting the fresh water away from the shelf.

[7] This paper identifies the pathways by which fresh water discharged by large rivers in the northern GoM is exported out of the region. The work also further examines the seasonal variability of the circulation in the northern GoM in connection with these export pathways using surface drifter data, historical hydrographic data, and data from a numerical model, the Navy Coastal Ocean Model (NCOM). This high-resolution numerical simulation permits the examination of coastally attached jets, large salinity gradients, and interaction of the buoyant water with the rich eddy field of the offshore environment.

[8] The NCOM and its application to the GoM region are described for the first time in this paper. Next, the model data, along with observational data, are used to demonstrate the existence of an annual cycle of surface salinity and in the along-shelf wind-driven currents over and near the continental shelf in the northern GoM. The role of the seasonally varying wind-driven transport of the low-salinity water is investigated as a mechanism for exporting low-salinity water from near the coast to regions where it is transported across the shelf break to the open ocean through interaction with the mesoscale eddy field.

2. Model

[9] The experiments conducted for this study were performed with a numerical simulation of the Gulf of Mexico that uses the NCOM [*Martin*, 2000]. The NCOM has been developed at the Naval Research Laboratory (NRL) for use in a coupled ocean-atmosphere model for simulating mesoscale and coastal regions [*Hodur et al.*, 2002]. The NCOM is similar in its physics and numerics to the Princeton Ocean Model (POM) [*Blumberg and Mellor*, 1987], but has some differences and some additional physical and numerical options. The model is relatively new, but is currently being used to simulate domains spanning from the global ocean to rather small-scale coastal and estuarine regions [*Martin*, 1999; *Hodur et al.*, 2002; *Rhodes et al.*, 2002].

[10] A notable difference from POM is the use of a hybrid vertical coordinate that was used in another model, the Sigma/Z-Level Model [*Martin et al.*, 1998]. This coordinate system uses sigma layers near the surface and geopotential (z) level vertical coordinates below a specified depth. This provides some flexibility in setting up the vertical grid. The model can be run with a full sigma or z-level grid (though at least one sigma layer is required to accommodate the free surface), or sigma layers can be used in the shallow water, for example, on the shelf, and z-levels, which are more robust to steep bathymetry, can be used in the deeper water including the steep shelf break region. A more detailed discussion of this hybrid vertical coordinate and its consequences is given by *Martin et al.* [1998], *Martin* [2000], and *Morey and O'Brien* [2002].

[11] The NCOM is a three-dimensional primitive equation ocean model with the commonly used hydrostatic, incompressible, and Boussinesq approximations. The equations, in Cartesian coordinates, are

$$\frac{\partial u}{\partial t} = -\nabla \cdot (\mathbf{v}u) + Qu + fv - \frac{1}{\rho_0}\frac{\partial p}{\partial x} + F_u + \frac{\partial}{\partial z}\left(K_M \frac{\partial u}{\partial z}\right), \quad (1)$$

$$\frac{\partial v}{\partial t} = -\nabla \cdot (\mathbf{v}v) + Qv - fu - \frac{1}{\rho_0}\frac{\partial p}{\partial y} + F_v + \frac{\partial}{\partial z}\left(K_M \frac{\partial v}{\partial z}\right), \quad (2)$$

$$\frac{\partial p}{\partial z} = -\rho g, \quad (3)$$

$$\nabla \cdot \mathbf{v} = \frac{\partial u}{\partial x} + \frac{\partial v}{\partial y} + \frac{\partial w}{\partial z} = Q, \quad (4)$$

$$\frac{\partial T}{\partial t} = -\nabla \cdot (\mathbf{v}T) + QT + \nabla_h (A_H \nabla_h T) + \frac{\partial}{\partial z}\left(K_H \frac{\partial T}{\partial z}\right) + Q_r \frac{\partial \gamma}{\partial z}, \quad (5)$$

$$\frac{\partial S}{\partial t} = -\nabla \cdot (\mathbf{v}S) + QS + \nabla_h (A_H \nabla_h S) + \frac{\partial}{\partial z}\left(K_H \frac{\partial S}{\partial z}\right), \quad (6)$$

$$\rho = \rho(T, S, z). \quad (7)$$

The variable Q in the above equations is a volume source/sink term that can be used to specify river and runoff inflows. The other variables are described in the notation section. The form of these equations in sigma coordinates is given by *Blumberg and Mellor* [1987].

[12] The surface boundary conditions are the surface stress for the momentum equations (1) and (2), the surface heat flux for the heat equation (5), and the effective surface salt flux for the salinity equation (6). The bottom stress for the momentum equations is parameterized by a quadratic drag law, and the fluxes of heat and salt at the bottom are set to zero. The density equation (7) is computed using the *Friedrich and Levitus* [1972] or *Mellor* [1991] formulations.

[13] The horizontal friction terms F_u and F_v are calculated using the Laplacian form of horizontal mixing with the mixing coefficients computed via the *Smagorinsky* [1963] scheme or a grid-cell Reynolds number scheme where the mixing coefficients are determined from a specified grid-cell Reynolds number. A minimum value of the mixing coefficient can be specified for either scheme. Vertical mixing is computed using the Mellor-Yamada Level 2 [*Mellor and Yamada*, 1974] or Level 2 1/2 [*Mellor and Yamada*, 1982] parameterizations. The surface roughness and, for the Level 2 1/2 mixing, the surface flux of turbulent kinetic energy, can be specified as by *Craig and Banner* [1994].

[14] The model equations are solved on the Arakawa C grid. The horizontal grid is orthogonal, and curvilinear as used in POM [*Blumberg and Herring*, 1987]. Spatial differences and interpolations are second or optionally fourth order. There are also options for quasi-third-order upwind advection for momentum and scalar fields [*Holland et al.*, 1998] and for flux-corrected transport (FCT) advection for scalar fields [*Zalesak*, 1979]. Temporal differencing is leapfrog with an *Asselin* [1972] filter to suppress timesplitting. The free surface and vertical mixing are treated implicitly; the other terms are treated explicitly. Shrink-wrapping is used in the x-grid dimension to skip

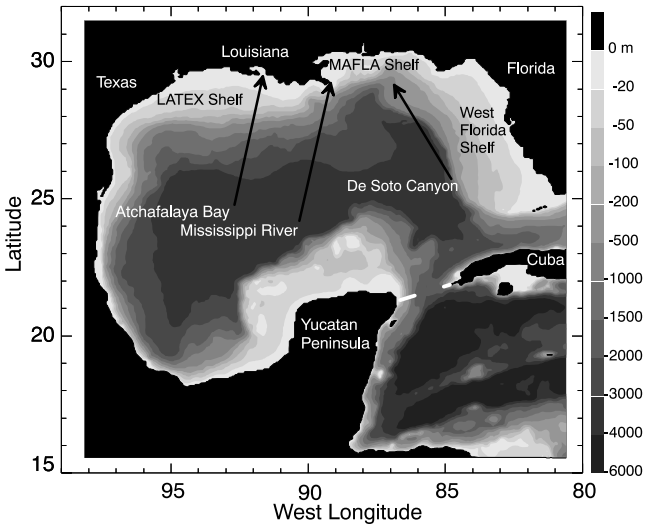

Figure 1. NCOM Gulf of Mexico simulation domain and topography. The dotted line between the Yucatan Peninsula and Cuba shows the section plotted in Figure 3.

calculations over land on the sides of the domain, and the model calculation proceeds through the domain in *x-z* slices to reduce the flushing of high-speed cache memory. NCOM is scaleable on a variety of multiprocessor computers and uses MPI, SHMEM, or OpenMP for interprocessor communication.

3. Gulf of Mexico Simulation

[15] The NCOM has been configured to simulate the entire GoM and the northwestern Caribbean with a horizontal resolution of 0.05° in latitude and longitude between like variables. The 352 × 320 horizontal grid encompasses 98.15°W–80.60°W, 15.55°N–31.50°N (Figure 1). Open boundaries are found along the eastern edge of the domain, in the Caribbean and the Florida Straits. This simulation has 20 evenly spaced sigma levels above 100 m depth and 20 z-levels below 100 m with stretched grid spacing to a maximum depth of 4000 m. Experiments using this GoM simulation are used for other studies involving a variety of deep ocean and shelf processes in the Gulf, and in research using high-frequency forcing. The experiments for this present study, however, use only climatological forcing. For this application, the NCOM is run using the Mellor-Yamada Level 2 turbulence closure scheme for vertical mixing, quasi-third-order upwind advection of scalars and momentum, and second-order calculations of the vertical advection terms, horizontal pressure gradient terms, and interpolations of the Coriolis term.

[16] Model initial temperature and salinity fields are derived from the 1994 World Ocean Atlas [*National Oceanic and Atmospheric Administration*, 1994] (WOA94). Surface forcing fields of wind stress, latent, sensible, and radiative heat fluxes are derived from the *DaSilva et al.* [1994] 0.5° × 0.5° analyzed COADS monthly climatology fields. A correction to the surface heat flux is applied to relax the model sea surface temperature to monthly climatology with a relaxation coefficient of 1 m/d (that is, a timescale in days proportional to the mixed layer depth in meters). There is no relaxation to climatological sea surface salinity. A surface salinity flux has the effect of uniformly evaporating water at a rate equal to the annual average combined discharge rates of the model rivers. Thirty rivers are simulated by using the volume flux source term in the model equations, with a salinity of 5 PSU and a temperature equal to the climatological sea surface temperature of the ocean at each location. Discharge rates for the United States rivers are derived from USGS gauging stations monthly averages, and discharge rates for the Mexican rivers are constant in time with annual averages taken from multiple sources. Two experiments using the model are run, one with time-constant river discharge, and another with monthly varying river discharge rates where available. All time-varying forcing fields for the model are linearly interpolated in time at each model time step.

[17] Inflow at the open boundaries is relaxed to temperature and salinity fields derived from the WOA94 monthly climatology data, and to a baroclinic velocity profile dynamically consistent with the WOA94 fields. The transport is calculated from a mean dynamic topography [*Fox et al.*, 2001] relative to 1000 m from historic hydrographic measurements. The *Orlanski* [1976] radiation condition is used at the open boundary with an upwind correction applied to the baroclinic normal velocity.

[18] The simulation is initialized from rest and run for 10 years with climatological forcing. The first of the Loop Current Eddies (LCEs) discussed below have reached the western continental margin within the first year of model integration and begin to decay. Model data are used for the study beginning in the fourth year of model integration, yielding 7 years of model data for both the experiment with constant river discharge and the experiment with climatological river discharge. In these experiments, output fields are saved every 48 hours for analysis.

4. Characteristics of the Model Solution

[19] Large-scale circulation features in the GoM, such as the well-known LC system and the associated eddies, are present in the numerical simulation (Figure 2). The westward Caribbean current enters through the eastern open boundary in the Caribbean Sea before turning northward and flowing into the GoM through the Yucatan Strait. This western boundary current penetrates northward into the GoM as the LC, which turns southward and eastward to flow out of the domain between the Florida Peninsula and Cuba as the Florida Current. The northern penetration of the LC in the model mean is approximately 26.5°N, compared to 27°N from a mean dynamic topography relative to 1000 m [*Fox et al.*, 2001], and compared to the average position of the LC northern boundary of approximately 27.5°N calculated from 5 years of satellite data [*Vukovich*, 1988a, 1988b].

[20] The transport of the LC, measured between the Yucatan Peninsula and Cuba, is 32 Sv (10^6 m s^{-1}) in the model, which is somewhat higher than previous estimates of 28 Sv [*Gordon*, 1967; *Roemmich*, 1981] and 23.8 Sv measured by *Sheinbaum et al.* [2002]. This discrepancy in transport can be addressed by changing the open boundary forcing based on other data sources for future simulations.

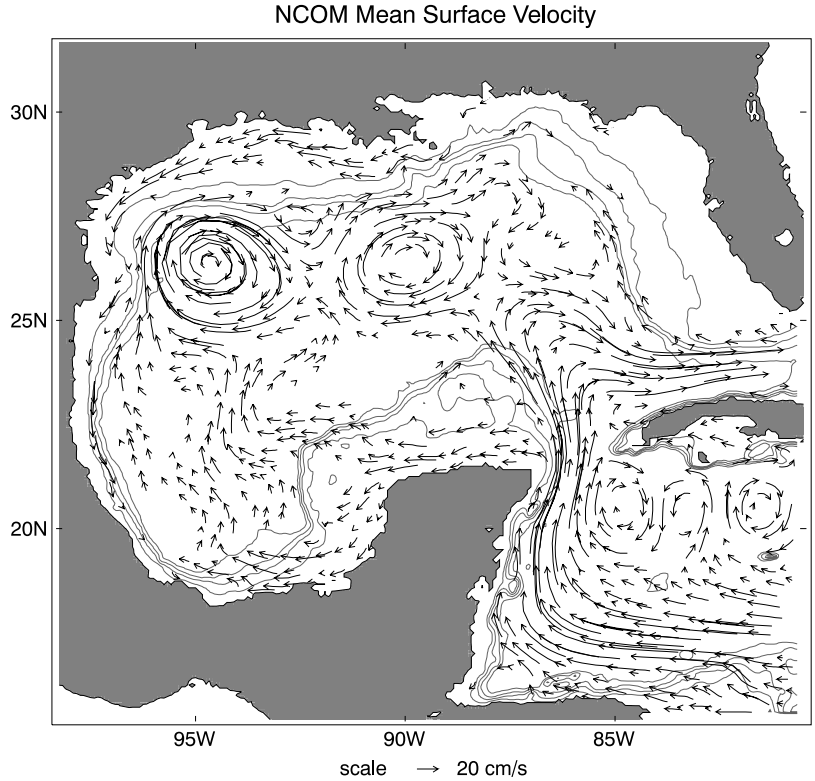

Figure 2. NCOM mean surface layer currents computed from 7 years of model integration. Vectors are randomly distributed with nearly uniform density, so not all grid points are shown. Vectors less than 5 cm/s are not drawn. The 50-m, 200-m, 500-m, and 1000-m isobaths are shown.

The structure of the Yucatan Channel flow in the model has similar characteristics to that reported by *Sheinbaum et al.* [2002]. The Yucatan current is confined to the upper 800 m with an undercurrent along the western continental slope and a weaker countercurrent along the Cuban coast with two cores, one in the upper 200 m and the other between 500 and 1000 m (Figure 3).

[21] The LC sheds large anticyclones at irregular intervals, a process of much discussion in the literature [e.g., *Hurlburt and Thompson*, 1982; *Pichevin and Nof*, 1997].

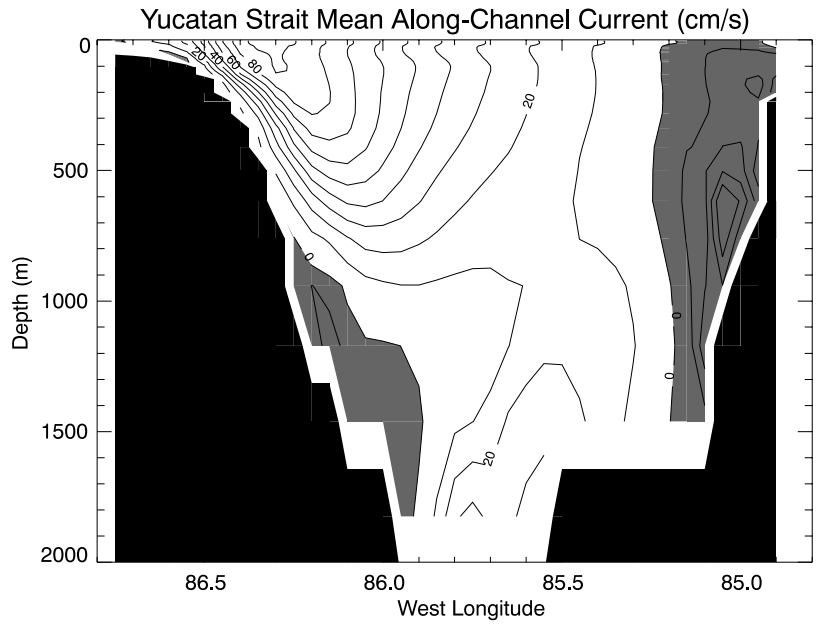

Figure 3. Yucatan Strait along-channel component of the mean velocity (positive toward the Gulf of Mexico). Positive contours are drawn every 20 cm/s, and negative contours (shaded regions) are drawn every 5 cm/s.

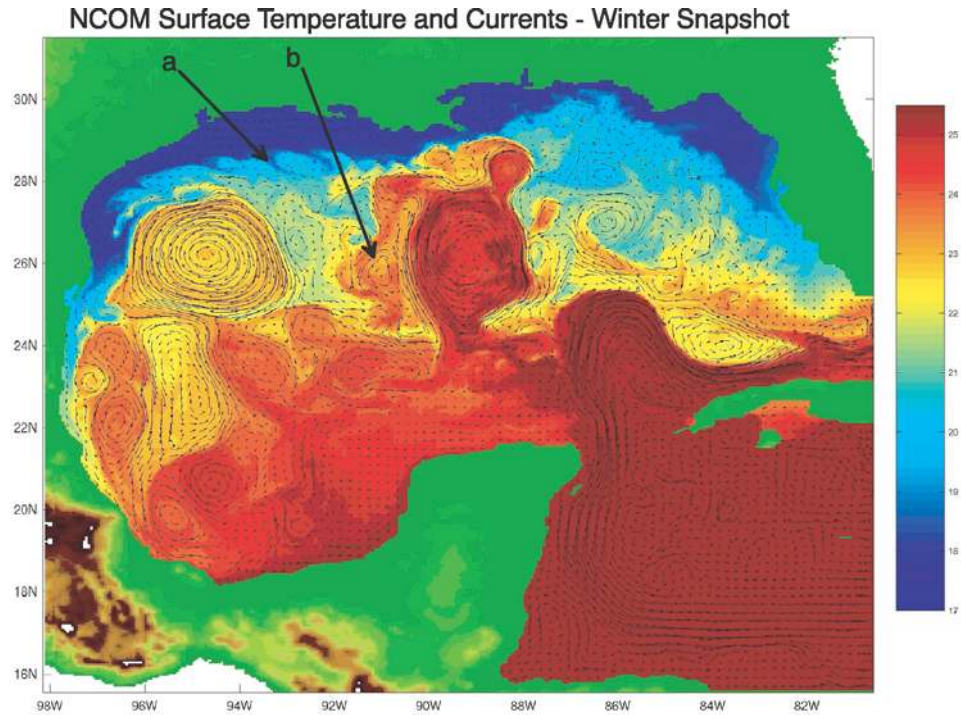

Figure 4. NCOM surface layer currents and temperature from an arbitrary output record during the winter season. Arrows point to examples of (“a”) filaments of cool water suggestive of frontal instabilities and (“b”) cyclonic frontal or “shingle” eddies surrounding an anticyclonic Loop Current Eddy.

These familiar LCEs drift generally westward, where they decay against the western continental margin, or possibly merge with existing anticyclonic features in the western Gulf. In the model, the LCEs follow more preferentially a northern pathway, similar to that of Eddy V in 1992–1993 reported by *Hamilton et al.* [1999] with less north-south variability of pathways than observed. Of 168 months of model data from the two model experiments, 17 LCEs were identified giving an average eddy shedding period of 9.9 months. *Sturges and Leben* [2000] reported a mean value of 9.5 months. As reported from observations, the eddy shedding periods in the model are not distributed closely about the mean. The shedding periods range from 2.7 to 15 months, which is consistent with the aperiodicity of the eddy shedding that has been previously reported.

[22] The model simulates other smaller scale circulation features that compare well to those seen in observations. These include smaller cyclones traveling along the LC front, called Loop Current Frontal Eddies or Shingle Eddies [*Fratantoni et al.*, 1998; *Zavala-Hidalgo et al.*, 2003a], jets between interacting eddy pairs [*Gilbes et al.*, 1996; *Sahl et al.*, 1997; *Muller-Karger*, 2000], and frontal instabilities along the continental shelf in the winter, all with spatial scales comparable to those seen in satellite thermal or chlorophyll images (Figure 4).

5. Model Seasonal Variability

[23] Seasonal variability in the surface salinity (actually, depth-averaged salinity in the topmost grid cell) spatial pattern is easily recognizable in animations of the model solution. The model is forced by monthly climatology fluxes, yet there is significant interannual variability due to the aperiodic LC eddy shedding and the energetic nonlinear eddy field. Nevertheless, certain features are consistently characteristic of particular seasons.

[24] Occasionally, jets of low-salinity water can be seen flowing offshore of the continental shelf across the shelf break toward the deep water of the central Gulf of Mexico. These features seem more evident east of the Mississippi Delta in the spring and summer, and off the Texas and northern Mexican shelf in the fall and winter (Figure 5). Also evident in the model snapshots are the spreading of the low-salinity water to the east of the Mississippi Delta in the summer and the appearance of coastally trapped low-salinity water on the LATEX and northern Mexican shelf in the winter. A similar pattern can be seen in satellite thermal images in the winter, as the coastal low salinity water is much cooler than the offshore water [*Zavala-Hidalgo et al.*, 2003b].

[25] In the model, the buoyant low-salinity water is confined to the coast and weakly stratified over the LATEX shelf in the fall and winter, yet spreads offshore as a strongly stratified freshwater cap over the broad shelf water during the summer (Figure 6). The model stratification patterns agree qualitatively with the salinity transects shown by *Wiseman et al.* [1997], while the horizontal salinity distribution is consistent with the salinity maps shown by *Cochrane and Kelly* [1986]. Over the Mississippi/Alabama/Florida (MAFLA) shelf, fresh water is more abundant during the summer and is similarly surface trapped.

[26] Monthly climatology of the model surface salinity shows a similar east-west pattern on the shelf in the northern

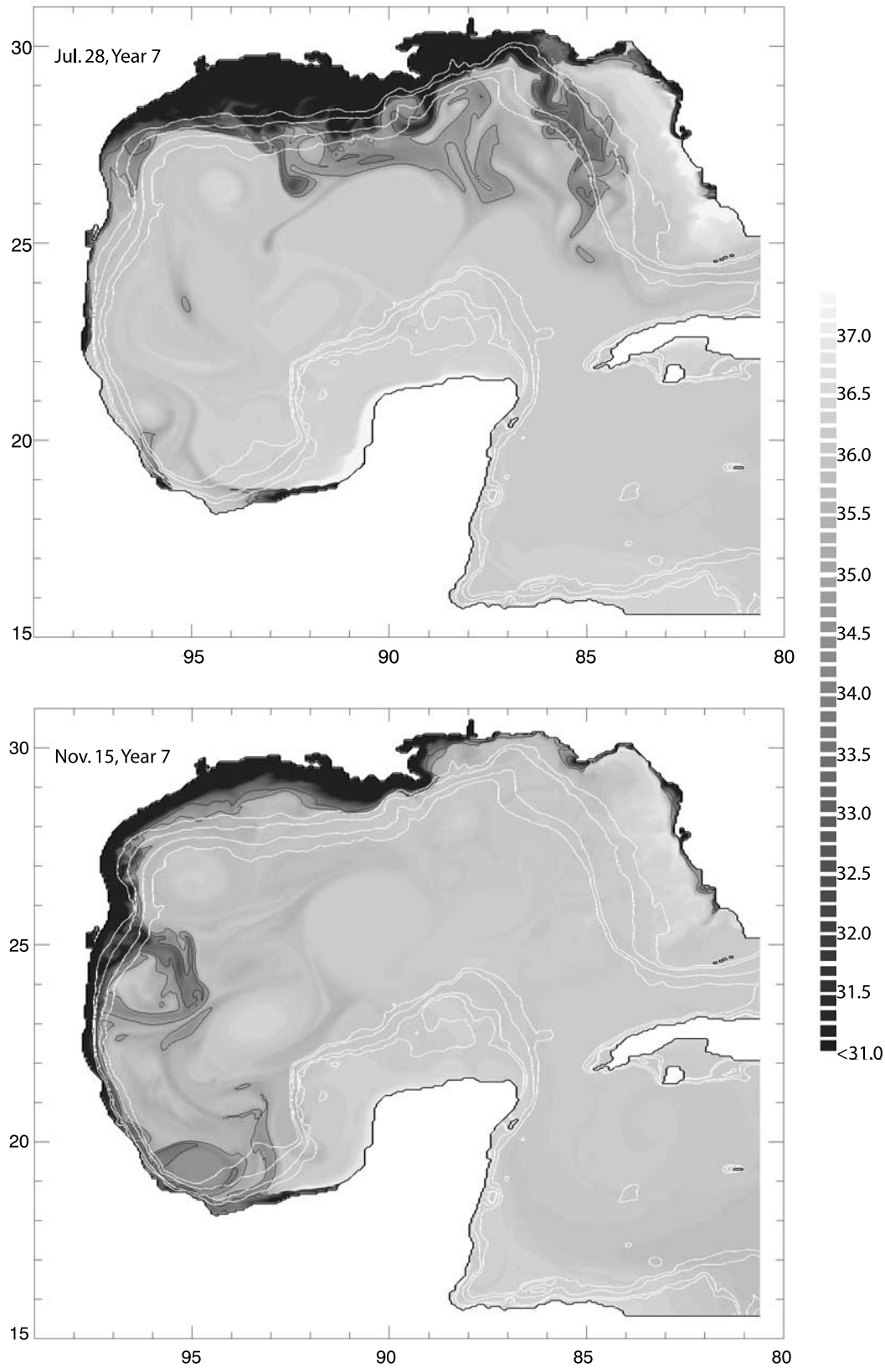

Figure 5. NCOM surface layer salinity from arbitrarily selected output records in the summer and late fall. The 34 and 35 PSU salinity contours are drawn, as are the 50-m, 200-m, 500-m, and 1000 m isobaths.

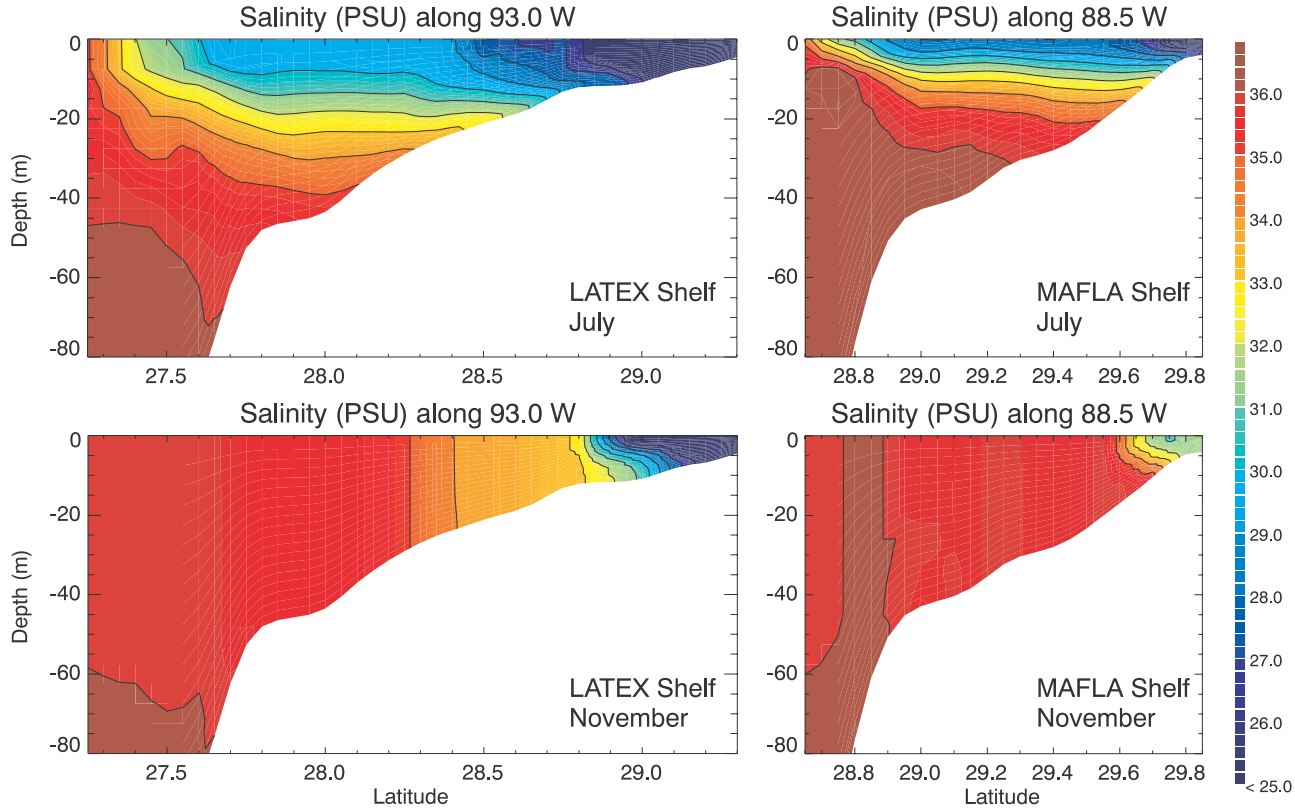

Figure 6. Model salinity sections for the upper 80 m along (left) 93°W and (right) 88.5°W from the coastline out to the 200-m isobath. The sections are plotted for arbitrarily chosen model output records from (top) July and (bottom) November. The scales are identical for each plot, and solid contour lines are drawn every 1 PSU.

Gulf (Figure 7). The MAFLA shelf region is much more saline in the fall (and not shown, but also throughout the winter) than in the summer when the low-salinity water from near the Mississippi River discharge location spreads eastward. Over the LATEX shelf, the low-salinity water is trapped very close to the coast extending all along the western boundary in the fall (again, through winter), and retreats spreading out over the shelf in the summer. The annual signal of salinity is verified by the near-surface (10 m) salinity climatology from the 1998 World Ocean Atlas (WOA98) [*Conkright et al.*, 1998] (Figure 8). Over the shelves, the model annual cycle of surface salinity agrees with the WOA98 values in the experiments with monthly varying river discharge, and with time constant river discharge. This indicates that the seasonal variability of river discharge is not the controlling mechanism for the annual cycle seen in the upper ocean salinity field in the northern GoM. Calculations with model data in the following sections will use data from the experiment with monthly varying river discharge.

6. Surface Drifters

[27] The seasonal variability of circulation patterns in the northern GoM is examined to help explain the seasonality of the export pathways for fresh water. Surface drifter trajectories from the SCULP I, SCULP II, and LATEX projects (provided by Walter Johnson, Minerals Management Service) are analyzed to find evidence of variability in the shelf circulation in the northern Gulf. The drifter trajectories used here are from drifters with drogue depths of 1 m below the surface.

[28] The satellite-tracked surface drifters were deployed at various locations on the LATEX shelf and the MAFLA shelf [*Yang et al.*, 1999; *Ohlmann et al.*, 2001]. For this present study, though, the drifter trajectories are not necessarily analyzed from their deployment positions and times, but are instead grouped using other criteria. Subsets of the surface drifter trajectories are selected based on the drifters' existence within a defined region during a particular month of any year. The first time a buoy is found to have a location within a prescribed region and time of year is taken as its new "pseudo-deployment" position and time for this study. Its subsequent trajectory is tracked for the time period under consideration. This approach allows a larger number of drifter trajectories to be analyzed for some indication of seasonal variability without necessarily being constrained to the drifters' actual deployment times and locations. Four calculations are conducted to include summer and winter seasons on both the MAFLA and LATEX shelves. The selection regions are: MAFLA Shelf, 89°W to 86.5°W within the 200 m isobath; and LATEX Shelf, 95°W to 91°W within the 200-m isobath. Drifters existing with these defined regions during June–July of any year are considered as "deployed" during the summer. Drifters existing in the regions during November–December are considered as part of the winter pseudo-deployments (Table 1). The drifters are tracked through the end of August for the summer experiments, and through the end of January for the winter

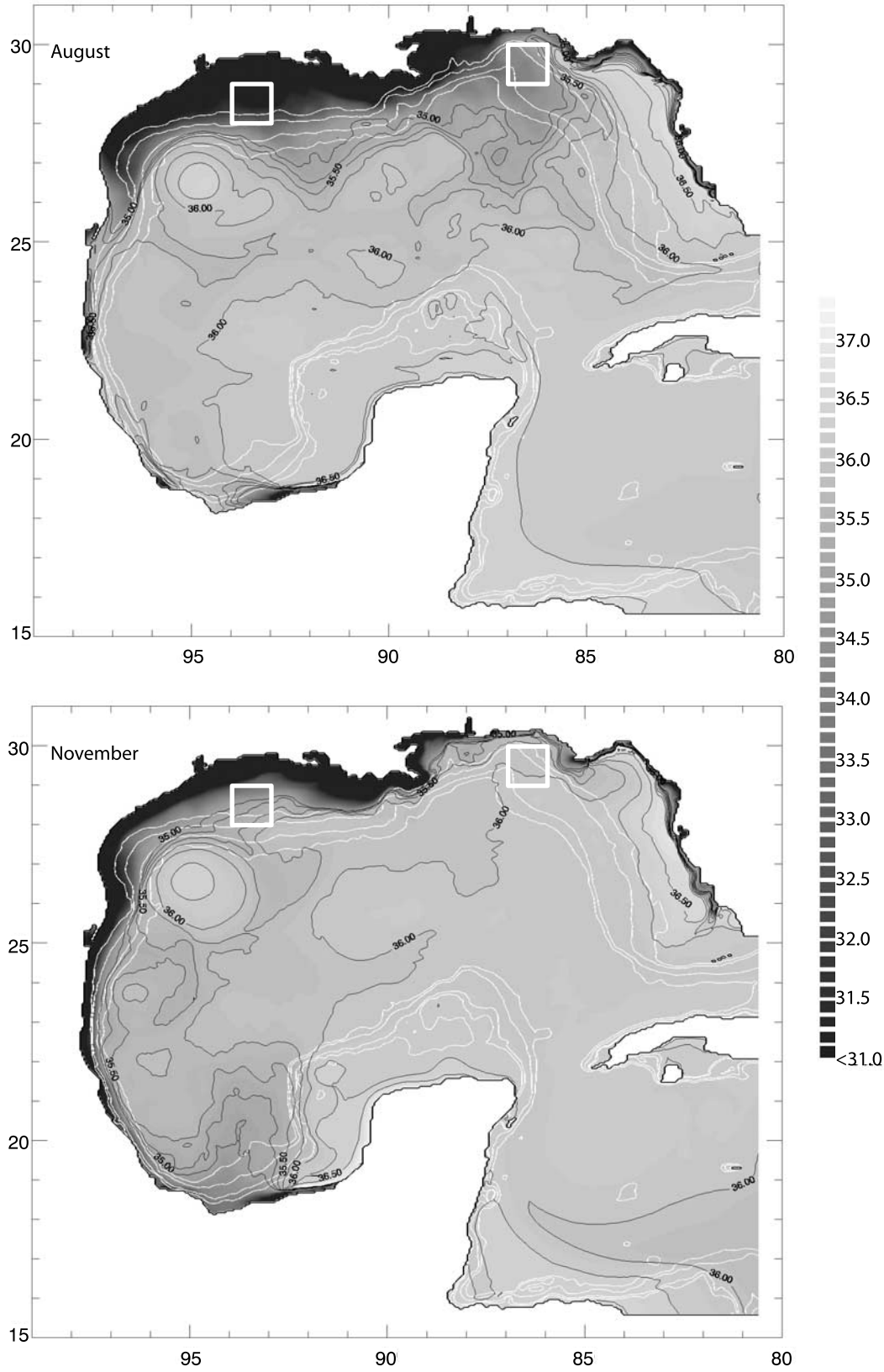

Figure 7. NCOM mean surface layer salinity (PSU) for August and November computed from seven years of model integration. The 50 m, 200 m, 500 m, and 1000 m isobaths are shown as white contour lines. The white boxes indicate the $1^\circ \times 1^\circ$ boxes over which the salinity is averaged for the plots in Figure 7.

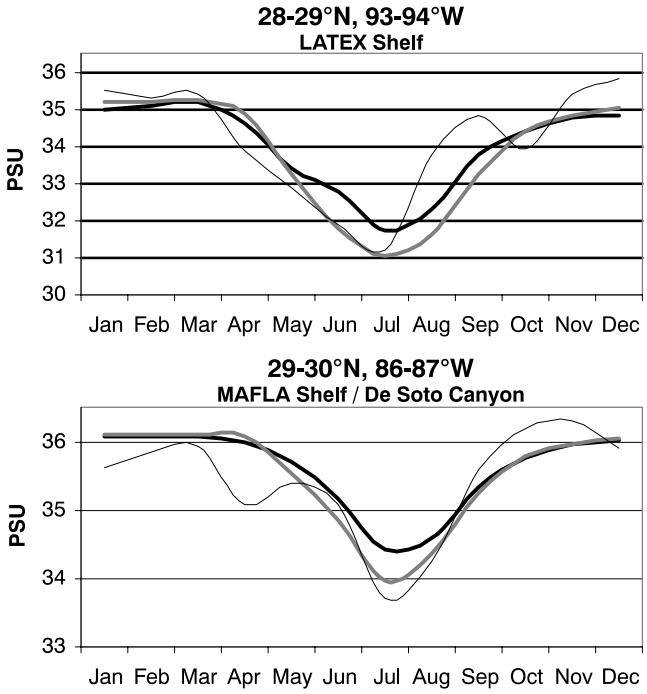

Figure 8. Monthly climatology salinity averaged over the $1^\circ \times 1^\circ$ boxes shown in Figure 6. Thin black line: World Ocean Atlas 1998 data vertically interpolated to the model surface grid cell depth average for the box. Thick black line: Surface grid cell salinity computed from 7 years of model integration with time constant river discharge. Thick shaded line: Surface grid cell salinity computed from 7 years of model integration with monthly varying river discharge.

experiments. Although the drifter tracks may be selected from any calendar year without regard of their actual deployment date, the drifter release dates and locations will still yield subsets of trajectories biased toward a particular year (as shown in Table 1). Because of the potential influence of interannual variability, this drifter trajectory analysis cannot be intended to produce an accurate picture of the shelf circulation climatology, but instead must be used only to provide evidence for a seasonal signal that can support the numerical model results and clarify the climatological signals seen in the historical hydrographic data.

[29] The drifter trajectories show clear evidence of seasonally varying surface circulation patterns (Figure 9). Over the LATEX shelf in the winter, drifters are seen flowing westward and southward along the Texas and Mexico coastline, where a large number cross the shelf break to the open ocean. Some are seen crossing the shelf break of the LATEX shelf, as well. In the summer, the drifters remain on the LATEX shelf, suggesting little export of shelf water from this location during this time of year. Over the MAFLA shelf, the drifters find their way westward onto the LATEX shelf during the winter. During the summer, the trajectories shift to the east. A number are seen crossing the shelf break and drifting toward the Florida Strait along the outer edge of the WFS continental slope. Some appear to flow onto the WFS.

[30] To quantitatively analyze these drifter migrations, the trajectories are followed and the net numbers of drifters exiting a larger defined region across various line segments are counted. For the LATEX shelf, this test region is divided as: along 27.5°N from the coastline eastward to 96°W (the 200 m isobath), along 27.5°N from 96°W to 90°W, and along 90°W from the coastline southward to 27.5°N. For the MAFLA shelf, the test region is divided as: along 89.5°W from the coastline southward to 28°N, along 28°N from 89.5°W to 85.5°W, and along 85.5°W from the coastline southward to 28°N (Figure 10).

[31] A striking example of the seasonal variability of the export of LATEX shelf water is seen along the western boundary of the domain. During the winter months, a large majority of the drifters leaving the test region exit southward very close to the coastline. These drifters are trapped in a southward flowing coastally attached wintertime current. This current has been documented by *Cho et al.* [1998] and has been shown to be relatively fresh [*Zavala-Hidalgo et al.*, 2003b]. This Lagrangian study supports the hypothesis that this water attains its properties on the LATEX shelf where it is influenced by the Atchafalaya and Mississippi Rivers. A secondary export pathway southward across the LATEX shelf break in the winter is suggested. No drifters pass eastward out of the test domain during the winter. During the summer, most of the drifters remain within the LATEX shelf region. There is little export of the shelf water at this time of year, although there is some evidence of a weak transport eastward out of the region. Data presented by *Cho et al.* [1998] show a generally eastward flow south of Louisiana during this June through August time period consistent with the summer circulation inferred here from the drifter trajectories.

[32] Over the MAFLA shelf in the winter, a large number of drifters are observed to exit the test region westward, past the Mississippi Delta, and onto the LATEX shelf. During the summer there is nearly no westward transport out of the test region, yet there is clear evidence of eastward transport. Since the major contributor of fresh water in the region, the Mississippi River, is located to the west of the pseudo-deployment region, it is reasonable to expect that the water near the MAFLA shelf is more saline during the winter and freshened in the summer as a result of eastward transport of the fresh water discharged by the river. This pattern is supported by recent surface salinity synoptic observations made during the Minerals Management Service sponsored Northeastern Gulf of Mexico (NEGOM) cruises [*Jochens et al.*, 2002].

7. Fresh-Water Flux

[33] The surface drifter trajectories suggest pathways for exporting shelf water from the region. These are not necessarily all export pathways for river-discharged fresh

Table 1. Number of Drifter Trajectory Segments From Each Calendar Year Included in the Drifter Trajectory Analyses Pseudo-Deployments

	1993	1994	1995	1996	1997	1998	1999
LATEX Shelf -Winter	95	16	0	39	0	0	0
LATEX Shelf -Summer	14	64	0	1	0	0	0
MAFLA Shelf -Winter	0	0	0	81	3	4	3
MAFLA Shelf -Summer	0	0	0	71	3	8	0

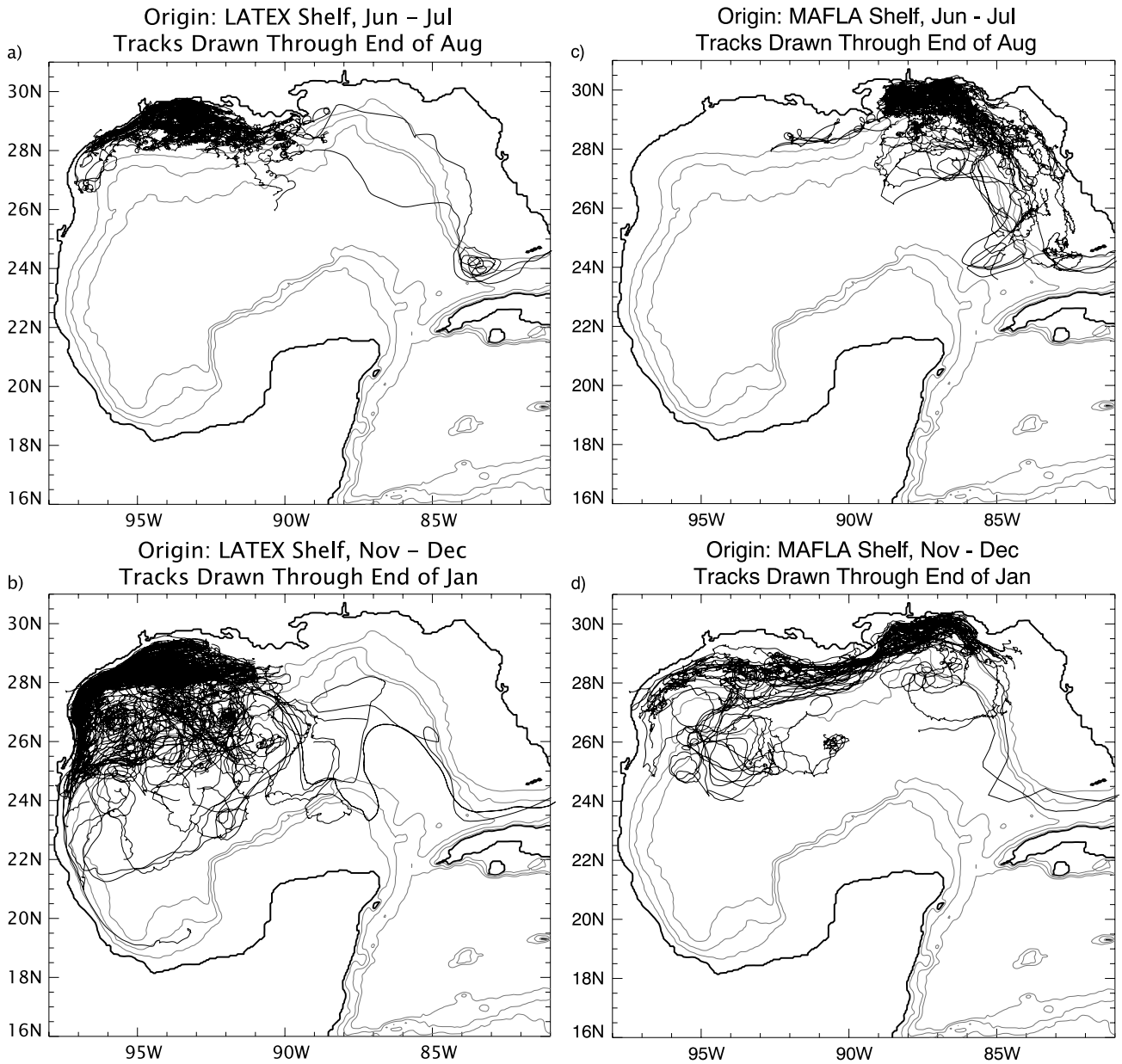

Figure 9. Trajectories for combined LATEX, SCULP I, and SCULP II 1-m drogued drifters. (a) Drifters existing within the defined LATEX shelf region in the summer months. (b) Drifters existing within the defined LATEX shelf region in the winter months. (c) Drifters existing within the defined MAFLA shelf region in the summer. (d) Drifters existing within the defined MAFLA shelf region in the winter. The 200-m, 1000-m, and 2000-m isobaths are drawn, shown by the shaded contour lines.

water. At times, the shelf water is rather saline, and not influenced by the river discharge. The numerical simulation has been shown to reproduce the characteristic circulation features of the GoM and the seasonal variability of salinity over the shelf, so it is used here to give an indication of the primary locations and times of year for cross-shelf export of the fresh water.

[34] A quantity proportional to the fresh-water flux per unit area in the direction of the unit vector **n** is defined as

$$F = u_{\mathbf{n}}(S_0 - S), \tag{8}$$

where $u_{\mathbf{n}}$ is the projection of the surface grid cell velocity vector onto **n**, S is the salinity, and S_0 is a reference salinity (taken as 36 PSU here). A freshwater export function can be defined as

$$E = \begin{cases} u_{\mathbf{n}}(S_0 - S), & u_{\mathbf{n}} \geq 0 \\ 0, & u_{\mathbf{n}} < 0 \end{cases}, \tag{9}$$

to examine the one-way transport of low salinity water across a given line. Equation (9) is computed (for the upper grid cells only) along a path following the 200-m isobath (where **n** is in the direction of the gradient of the positive ocean depth). Thus, positive values of E indicate cross-shelf export of fresh water. Equation (8) is computed and averaged

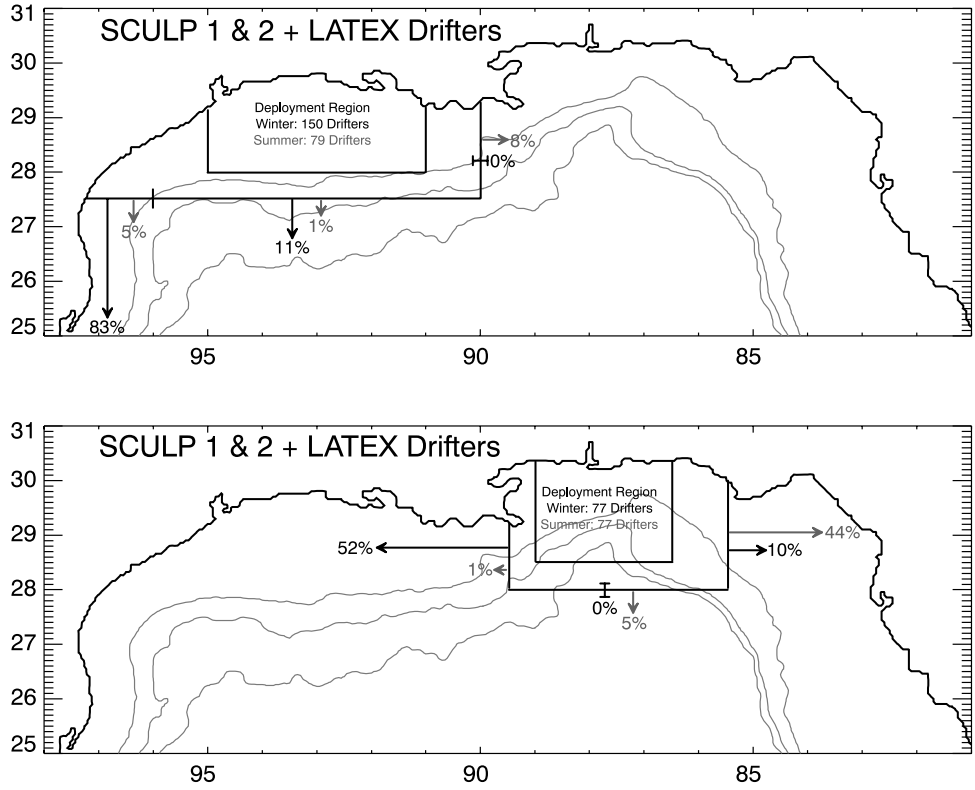

Figure 10. Schematic showing the net percentage of drifters initially existing within the defined deployment region during the prescribed months exiting the domain across the identified line segments. Note that the deployment region is shown by a box, but actually only extends out to the 200-m isobath. The 200-m, 1000-m, and 2000-m isobaths are drawn, shown by the shaded contour lines.

along some strategically placed cross-shelf line segments (where **n** is the normal vector to the line segment). The time series of E and F are constructed for 7 years of model data at 2-day intervals. The climatology of these time series show the preferred locations for transport of low salinity water at different times of the year (Figures 11 and 12).

[35] A dominant pathway for cross-shelf export in the northern GoM appears to the east of the Mississippi Delta, along the MAFLA shelf (Figure 11). This pathway is primarily active in the late spring through summer months. A secondary cross-shelf export pathway can be seen along the LATEX shelf, again in the summer. Although the drifters showed a more active cross-shelf transport here during the winter (Figure 10), the low-salinity water is confined to the coast at this time and is only found near the shelf edge during the summer (Figure 6) [*Cochrane and Kelly*, 1986]. At the very southwestern edge of the study region, cross-shelf export seems quite active. This is expected to occur even more so southward of the study domain along the Mexican coast where the shelf narrows allowing the decaying LCEs to penetrate very close to the coastline [*Zavala-Hidalgo et al.*, 2003b]. The preferred northern pathway for the model LCEs mentioned in section 4 may contribute to the secondary cross-shelf fresh water export pathway of the LATEX Shelf. This pathway is likely to exist, as LCEs have been shown to take very similar paths as those in the model (e.g., Eddy V of *Hamilton et al.* [1999]), but its importance may be overestimated in the numerical simulations.

[36] The along-shelf fresh-water flux is consistent with what was seen in the surface drifter trajectories. Fresh-water flux is westward onto the LATEX shelf during the entire year, except the summer months. Similarly, fresh-water flux eastward of the Mississippi River is seen only during the summer months. Little eastward fresh-water flux is seen to the east of the De Soto Canyon, even though a number of drifters found their way eastward onto the WFS in the summer. This is due to the fact that the water on the narrow shelf east of the De Soto Canyon is more saline than toward the west (Figures 5 and 7).

8. Discussion

[37] The model results and analysis of observational data show a clear annual signal in the upper ocean salinity field over the continental shelf in the northern GoM. A seasonal transition from eastward to westward transport of the low-salinity water from the spring and summer seasons to the fall and winter seasons has also been demonstrated. The model experiments with constant and climatological river discharge give similar results, indicating that the variability in river discharge does not control the seasonal variability of salinity in the region, away from the fresh-water sources. This suggests the residence time over the LATEX and MAFLA shelves is long enough to effectively filter out the large annual signal of the river discharge rates.

[38] The model can provide insight into the cause of the seasonal reversal of transport in the northern GoM. The

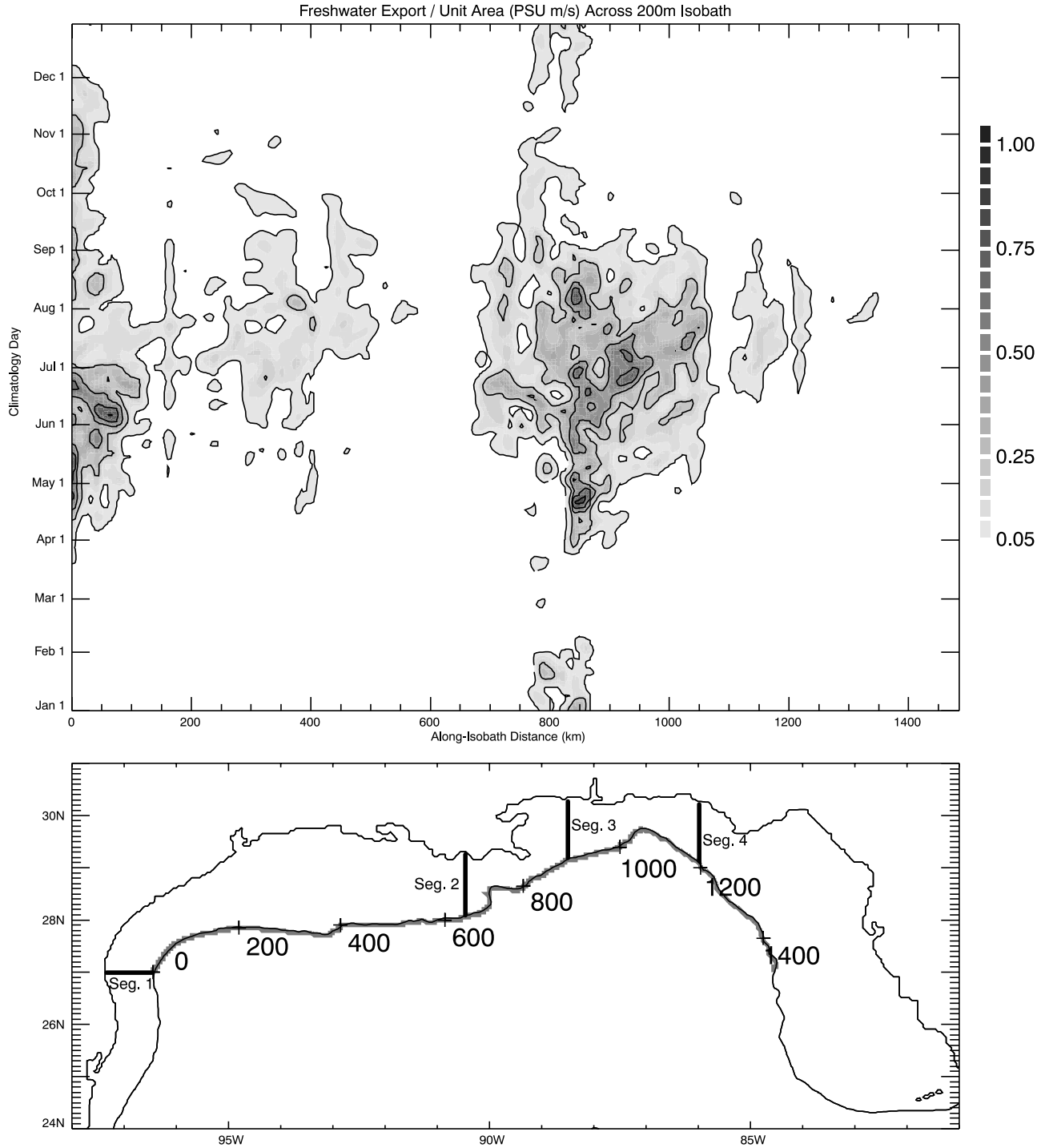

Figure 11. (top) Model climatology fresh water export per unit area, as approximated by equation (9), across the 200-m isobath as a function of along-isobath distance (shown at the bottom) and time. (bottom) The 200-m isobath used in the above calculation is highlighted with along-isobath distance indicated. The numbered cross-shelf line segments show the locations for the fresh-water flux climatology computed in Figure 11.

only seasonally varying forcing functions in the model are river discharge rates (in only one experiment), surface wind stress, and surface heat flux. The reversing current near the coast could possibly be wind driven or density driven. A density-driven current, however, would flow in the direction with less dense water to the right. Thus a density-driven westward/southward current on the LATEX shelf and along the Mexican coastline during the winter could be explained by a reduction of the density along the coast. However, the coastal waters are actually cooling faster than the offshore waters at this time of year, so the seasonal variability of heat flux is not the cause. Additionally, the current forms in both experiments with and without seasonally varying fresh water input, and the formation of the coastally attached

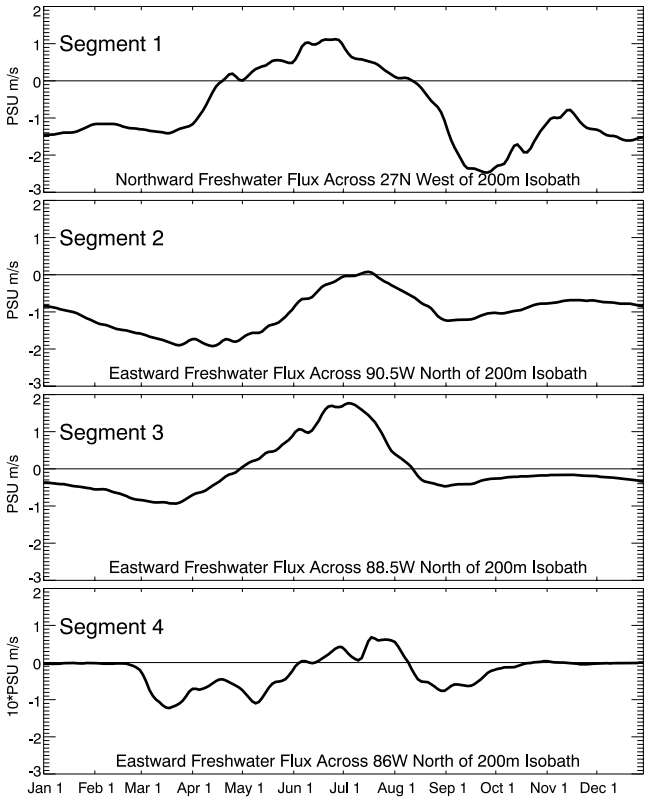

Figure 12. Model climatology fresh water flux per unit area (positive northward and eastward), as approximated by equation (8), across the numbered line segments shown in Figure 10. Note the different axis scaling for segment 4.

current, occurs just following the climatological minimum of river discharge in the northern GoM. Thus seasonal variability of fresh water input along the coast is not responsible. This leaves the seasonal shift in the climatological wind direction over the northern GoM from southeasterly in the spring and summer to northeasterly in the fall and winter as the mechanism responsible for the seasonally reversing transport.

[39] During the spring and summer months, as the surface water warms in the northern GoM, the water column becomes highly stratified, particularly in the region capped with the low-salinity water formed by river discharge. The salinity sections discussed previously (Figure 6) show a very stratified water column to the east of the Mississippi Delta in the summer. The Ekman transport in the surface layer will be to the right of the local wind stress vector. Southeasterly winds in the spring, shifting more southerly during the summer months, over the region east of the Mississippi Delta drive eastward Ekman transport in this low-salinity surface layer (Figure 13). That is, the transport within the buoyant surface layer of the stratified water column will be generally eastward resulting in the spreading of low-salinity water to the east of the fresh water source (i.e., the Mississippi River discharge). To the east of the Mississippi Delta, the shelf is relatively narrow and the low salinity water spreads toward the deep De Soto Canyon. Here, the low-salinity water can interact with the open ocean energetic mesoscale eddy field. Cyclones and anticyclones intruding into the De Soto Canyon can entrain this buoyant low-salinity water found near the shelf edge and transport it offshore as jets of low-salinity water (Figure 5) [*Morey et al.*, 2003].

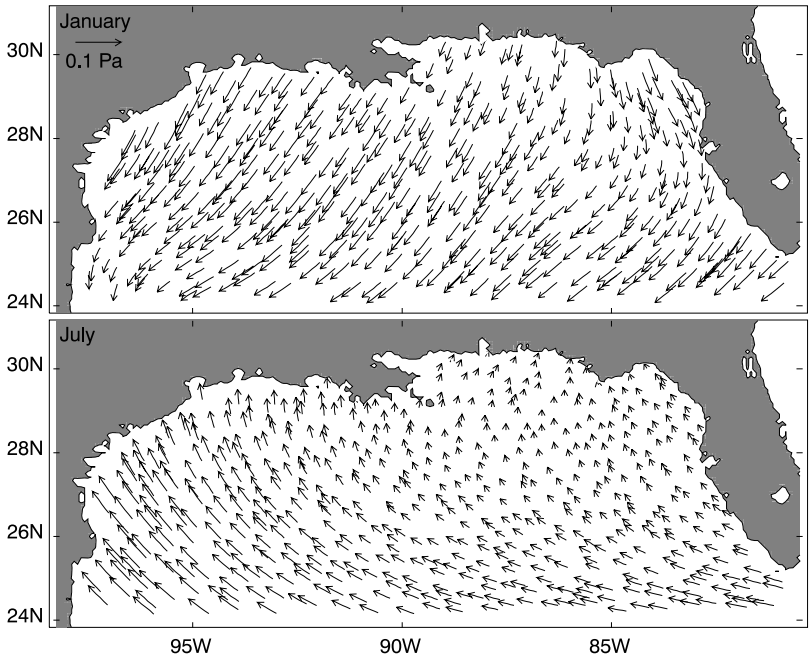

Figure 13. Monthly climatology wind stress derived from COADS [*DaSilva*, 1994] for (top) January and (bottom) July.

[40] In September, and continuing through the winter, the winds in the northern Gulf become easterly shifting to northeasterly and northerly in the northern GoM, consistent with a westward/southward coastal current (Figure 13). Over the northern Gulf, the winds become more variable during the fall and winter as the weather patterns are dominated by the passages of cold fronts. The strong northerly winds behind these fronts have the greatest influence on the wind climatology. Thus the westward/southward coastal transport actually occurs in an episodic nature coincident with these northerly wind events. It is likely that the smooth climatological winds may actually cause the model to underpredict the strength of this western export pathway. Similarly, occasional tropical storms in the region during the summer will also alter the export pathways during the events, but are likely so occasional so as not to significantly alter the climatological behavior of the pathways. Nevertheless, the strong consistency between the ocean model forced by climatological fields and the observational data presented here demonstrates the robustness of the description of the fresh water export pathways in the northern GoM.

9. Summary and Conclusions

[41] A new primitive equation ocean model has been described and applied to simulate the GoM ocean circulation. This numerical simulation, along with new calculations using existing observational data, have been used to determine the eventual fate of fresh water discharged by rivers in the northern Gulf. The export pathways, and their seasonal variability, for river discharged fresh water have been determined through the analysis of surface drifter data and numerical experiments. The seasonal reversal of the wind driven transport from westward in the fall and winter to eastward during the spring and summer shifts the locations of the export pathways.

[42] Analyses of surface drifters, and previous works [*Ohlmann et al.*, 2001], have shown the preferential locations for cross-shelf transport in the northern GoM. However, because of the seasonally shifting along-shelf transport of low-salinity water, not all cross-shelf transport results in fresh water export. The results of this study show that the export pathway during the late fall and winter consists of a westward/southward flowing coastal jet. It is likely that the fresh water exported as part of this jet is eventually transported across the shelf through entrainment into jets associated with deep water eddies south of the study region along the narrow Mexican shelf [*Zavala-Hidalgo et al.*, 2003b]. In the spring through summer, the buoyant low-salinity water is transported to the east where it finds its way out of the domain across the MAFLA shelf near the De Soto Canyon, again through interaction with the mesoscale eddy field of the Gulf.

Notation

x, y, z	coordinate directions.
t	time.
$\mathbf{v} = (u, v, w)$	three-dimensional vector velocity.
Q	volume flux source term.
T	potential temperature.
S	salinity.
∇_h	horizontal gradient operator.
f	Coriolis parameter.
p	pressure.
ρ	water density.
ρ_0	reference water density.
g	acceleration of gravity.
F_u, F_v	horizontal mixing terms for momentum.
A_h	coefficient of horizontal mixing for scalars.
K_M	vertical eddy coefficient for momentum.
K_H	vertical eddy coefficient for scalars.
Q_r	solar radiation.
γ	function describing extinction of solar radiation with depth.

[43] **Acknowledgments.** This project was sponsored by funding provided by the Office of Naval Research Secretary of the Navy grant awarded to James J. O'Brien, the ONR sponsored Distributed Marine Environment Forecast System, and by a NASA Office of Earth Science grant to the COAPS authors. Simulations were performed on the IBM SPs at Florida State University and the Naval Oceanographic Office. Computer time was provided by the DoD High Performance Computing Modernization Office, and by the FSU Academic Computing and Network Services. The authors thank Walter Johnson for supplying the SCULP and LATEX drifter data, and William Schroeder and Nobuo Suginohara for their advice.

References

Asselin, R., Frequency filter for time integrations, *Mon. Weather Rev.*, *100*, 487–490, 1972.

Blumberg, A. F., and H. J. Herring, Circulation modeling using orthogonal curvilinear coordinates, in *Three-Dimensional Models of Marine and Estuarine Dynamics*, *Elsevier Oceanogr. Ser.*, vol. 45, edited by J. C. Nihoul and B. M. Jamart, pp. 55–88, Elsevier Sci., New York, 1987.

Blumberg, A. F., and G. L. Mellor, A description of a three-dimensional coastal ocean circulation model, in *Three-Dimensional Coastal Ocean Models*, *Coastal Estuarine Stud.*, vol. 4, edited by N. Heaps, pp. 1–16, AGU, Washington, D. C., 1987.

Brooks, D. A., and R. V. Legeckis, A ship and satellite view of hydrographic features in the western Gulf of Mexico, *J. Geophys. Res.*, *87*, 4195–4206, 1982.

Cho, K., R. O. Reid, and W. D. Nowlin Jr., Objectively mapped stream function fields on the Texas-Louisiana shelf based on 32 months of moored current meter data, *J. Geophys. Res.*, *103*, 10,377–10,390, 1998.

Chuang, W., W. W. Schroeder, and W. J. Wiseman Jr., Summer current observations off the Alabama coast, *Contrib. Mar. Sci.*, *25*, 121–131, 1982.

Cochrane, J. D., and F. J. Kelly, Low-frequency circulation on the Texas-Louisiana continental shelf, *J. Geophys. Res.*, *91*, 10,645–10,659, 1986.

Conkright, M., S. Levitus, T. O'Brien, T. Boyer, J. Antonov, and C. Stephens, World Ocean Atlas 1998 CD-ROM data set documentation, *Tech. Rep. 15*, Natl. Oceanic and Atmos. Admin., Silver Spring, MD, 1998.

Craig, P. D., and M. L. Banner, Modeling wave-enhanced turbulence in the ocean surface layer, *J. Phys., Oceanogr.*, *24*, 2546–2559, 1994.

DaSilva, A., A. C. Young, and S. Levitus, *Atlas of Surface Marine Data 1994*, vol. 1, *Algorithms and Procedures*, *NOAA Atlas NESDIS 6*, Natl. Oceanic and Atmos. Admin., Silver Spring, Md., 1994.

Fox, D. N., W. J. Teague, C. N. Barron, M. R. Carnes, and C. M. Lee, The Modular Ocean Data Assimilation System (MODAS), *J. Atmos. Oceanic Technol.*, *19*, 240–252, 2001.

Fratantoni, P. S., T. N. Lee, G. P. Podesta, and F. Muller-Karger, The influence of loop current perturbations on the formation and evolution of Tortugas eddies in the southern Straits of Florida, *J. Geophys. Res.*, *103*, 24,759–24,779, 1998.

Friedrich, H., and S. Levitus, An approximation to the equation of state for sea water, suitable for numerical ocean models, *J. Phys. Oceanogr.*, *2*, 145–167, 1972.

Gilbes, F., C. Thomas, J. J. Walsh, and F. E. Muller-Karger, An episodic chlorophyll plume on the West Florida Shelf, *Cont. Shelf. Res.*, *16*, 1201–1224, 1996.

Gordon, A., Circulation of the Caribbean Sea, *J. Geophys. Res.*, *72*, 6207–6223, 1967.

Hamilton, P., G. S. Fargion, and D. C. Biggs, Loop Current eddy paths in the western Gulf of Mexico, *J. Phys. Oceanogr.*, *29*, 1180–1207, 1999.

Hodur, R. M., J. Pullen, J. Cummings, X. Hong, J. D. Doyle, P. Martin, and M. A. Rennick, The Coupled Ocean/Atmosphere Mesoscale Prediction System (COAMPS), *Oceanography*, *15*, 88–98, 2002.

Holland, W. R., J. C. Chow, and F. O. Bryan, Application of a third-order upwind scheme in the NCAR Ocean Model, *J. Clim.*, *11*, 1487–1493, 1998.

Hurlburt, H. E., and J. D. Thompson, The dynamics of the Loop Current and shed eddies in a numerical model of the Gulf of Mexico, in *Hydrodynamics of Semi-Enclosed Seas*, edited by J. C. J. Nihoul, pp. 243–298, Elsevier Sci., New York, 1982.

Jochens, A. E., S. F. DiMarco, W. D. Nowlin Jr., R. O. Reid, and M. C. Kennicutt II, Northeastern Gulf of Mexico Chemical Oceanography and Hydrography Study: Synthesis report, *OCS Study MMS 2002-055*, 586 pp., U.S. Dept. of the Interior, Minerals Manage. Serv., Gulf of Mex. OCS Reg., New Orleans, La., 2002.

Martin, P. J., An ocean model applied to the Chesapeake Bay plume, in *Estuarine and Coastal Modeling, Proceedings of the 6th International Conference*, edited by M. L. Spaulding and J. L. Butler, pp. 1055–1067, Am. Soc. of Civ. Eng., Reston, Va., 1999.

Martin, P. J., A description of the Navy Coastal Ocean Model Version 1.0, *NRL/FR/7322-009962*, 39 pp., Nav. Res. Lab., Stennis Space Center, Miss., 2000.

Martin, P. J., G. Peggion, and K. J. Yip, A comparison of several coastal ocean models, *NRL/FR/7322-97-9672*, 95 pp., Nav. Res. Lab., Stennis Space Center, Miss., 1998.

Mellor, G. L., An equation of state for numerical models of oceans and estuaries, *J. Atmos. Oceanic Technol.*, *8*, 609–611, 1991.

Mellor, G. L., and T. Yamada, A hierarchy of turbulence closure models for planetary boundary layers, *J. Atmos. Sci.*, *31*, 1791–1806, 1974.

Mellor, G. L., and T. Yamada, Development of a turbulence closure model for geophysical fluid problems, *Geophys. Space Phys.*, *20*, 851–875, 1982.

Morey, S. L., and J. J. O'Brien, The spring transition from horizontal to vertical stratification on a mid-latitude continental shelf, *J. Geophys. Res.*, *107*(C8), 3097, doi:10.1029/2001JC000826, 2002.

Morey, S. L., W. W. Schroeder, J. J. O'Brien, and J. Zavala-Hidalgo, The annual cycle of riverine influence in the eastern Gulf of Mexico basin, *Geophys. Res. Lett.*, *30*(16), 1867, doi:10.1029/2003GL017348, 2003.

Muller-Karger, F. E., The spring 1998 northeastern Gulf of Mexico (NEGOM) cold water event: Remote sensing evidence for upwelling and for eastward advection of Mississippi water (or: How an errant Loop Current anticyclone took the NEGOM for a spin), *Gulf of Mex. Sci.*, *1*, 55–67, 2000.

National Oceanic and Atmospheric Administration, *World Ocean Atlas 1994* [CD-ROM NODC-43], Natl. Oceanogr. Data Cent., Washington, D. C., 1994.

Ohlmann, J. C., P. P. Niiler, C. A. Fox, and R. R. Leben, Eddy energy and shelf interactions in the Gulf of Mexico, *J. Geophys. Res.*, *106*, 2605–2620, 2001.

Orlanski, I., A simple boundary condition for unbounded hyperbolic flows, *J. Comput. Phys.*, *21*, 251–269, 1976.

Pichevin, T., and D. Nof, The momentum imbalance paradox, *Tellus*, *Ser. A*, *49*, 298–319, 1997.

Rhodes, R. C., et al., Navy real-time global modeling systems, *Oceanography*, *15*, 29–43, 2002.

Roemmich, D., Circulation of the Caribbean Sea: A well-resolved inverse problem, *J. Geophys. Res.*, *86*, 7993–8005, 1981.

Sahl, L. E., D. A. Wiesenburg, and W. J. Merrrell, Interactions of mesoscale features with Texas shelf and slope waters, *Cont. Shelf. Res.*, *17*, 117–136, 1997.

Schroeder, W. W., O. K. Huh, L. J. Rouse Jr., and W. J. Wiseman Jr., Satellite observations of the circulation east of the Mississippi Delta: Cold air outbreak conditions, *Remote Sens. Environ.*, *18*, 49–58, 1985.

Schroeder, W. W., S. P. Dinnel, W. J. Wiseman Jr., and W. J. Merrell Jr., Circulation patterns inferred from the movement of detached buoys in the eastern Gulf of Mexico, *Cont. Shelf. Res.*, *7*, 883–894, 1987.

Sheinbaum, J., J. Candela, A. Badan, and J. Ochoa, Flow structure and transport in the Yucatan Channel, *J. Geophys. Res.*, *29*, doi:10.1029/2001GL013990, 2002.

Smagorinsky, J., General circulation experiments with the primitive equations: I. The basic experiment, *Mon. Weather Rev.*, *91*, 99–164, 1963.

Sturges, W., and R. Leben, Frequency of ring separations from the Loop Current in the Gulf of Mexico: A revised estimate, *J. Phys. Oceanogr.*, *30*, 1814–1819, 2000.

Vastano, A. C., C. N. Barron Jr., and E. W. Shaar Jr., Satellite observations of the Texas Current, *Cont. Shelf Res.*, *15*, 729–754, 1995.

Vukovich, F. M., On the formation of elongated cold perturbations off the Dry Tortugas, *J. Phys. Oceanogr.*, *18*, 1051–1059, 1988a.

Vukovich, F. M., Loop current boundary variations, *J. Geophys. Res.*, *93*, 15,585–15,591, 1988b.

Yang, H., R. H. Weisberg, P. P. Niiler, W. Sturges, and W. Johnson, Lagrangian circulation and forbidden zone on the West Florida Shelf, *Cont. Shelf Res.*, *19*, 1221–1245, 1999.

Wiseman, W. J., N. N. Rabalais, R. E. Turner, S. P. Dinnel, and A. MacNaughton, Seasonal and interannual variability within the Louisiana coastal current: Stratification and hypoxia, *J. Mar. Syst.*, *12*, 237–248, 1997.

Zalesak, S. T., Fully multidimensional flux-corrected transport algorithms for fluids, *J. Comp. Phys.*, *31*, 335–362, 1979.

Zavala-Hidalgo, J., S. L. Morey, and J. J. O'Brien, Cyclonic eddies northeast of the Campeche Bank from altimetry data, *J. Phys. Oceanogr.*, *33*, 623–629, 2003a.

Zavala-Hidalgo, J., S. L. Morey, and J. J. O'Brien, Seasonal circulation on the western shelf of the Gulf of Mexico, *J. Geophys. Res.*, doi:10.1029/2003JC001879, in press, 2003b.

S. L. Morey, J. J. O'Brien, and J. Zavala-Hidalgo, Center for Ocean-Atmospheric Prediction Studies, Florida State University, Tallahassee, FL 32306-2840, USA. (morey@coaps.fsu.edu; obrien@coaps.fsu.edu; zavala@coaps.fsu.edu)

P. J. Martin and A. A. Wallcraft, Naval Research Laboratory, Stennis Space Center, MS 39529-5004, USA. (martin@nrlssc.navy.mil; wallcraf@nrlssc.navy.mil)